Neuromorphic, Digital and Quantum Computation with Memory Circuit Elements

Yuriy V. Pershin and Massimiliano Di Ventra

Abstract—**Memory effects are ubiquitous in nature and the class of memory circuit elements - which includes memristive, memcapacitive and meminductive systems - shows great potential to understand and simulate the associated physical processes. Here, we show that such elements can also be used in electronic schemes mimicking biologically-inspired computer architectures, performing digital logic and arithmetic operations, and can expand the capabilities of certain quantum computation schemes. In particular, we will discuss some examples where the concept of memory elements is relevant to the realization of associative memory in neuronal circuits, spike-timing-dependent plasticity of synapses, digital and field-programmable quantum computing.**

Index Terms—**Memory, Resistance, Capacitance, Inductance, Dynamic response, Hysteresis.**

I. INTRODUCTION

MEMRISTIVE [1], [2], memcapacitive and meminductive [3] systems constitute an important class of two-terminal circuit elements whose basic characteristics - namely, their resistance, capacitance and inductance - retain memory of the past states through which the systems have evolved. The memory features of these systems are related to corresponding internal states of these elements (e.g., atomic structure [4], spin polarization [5], [6], etc.) which can be influenced by an external control parameter like the voltage, charge, current or flux.

Mathematically, nth-order u-controlled memory elements are defined by the relations [3]

$$y(t) = g(x, u, t) u(t) \quad (1)$$
$$\dot{x} = f(x, u, t) \quad (2)$$

where x denotes a set of n state variables describing the internal state of the system, $u(t)$ and $y(t)$ are any two fundamental circuit variables (i.e., current, charge, voltage, or flux) denoting input and output of the system, g is a generalized response, and f is a continuous n-dimensional vector function. The different memory elements are determined by three pairs of circuit variables: current-voltage (memristive systems), charge-voltage (memcapacitive systems), and flux-current (meminductive systems). Two other pairs (charge-current and voltage-flux) are linked through equations of electrodynamics, and therefore do not give rise to any new element. Devices defined by the relation of charge and flux

Yu. V. Pershin is with the Department of Physics and Astronomy and USC Nanocenter, University of South Carolina, Columbia, SC, 29208
e-mail: pershin@physics.sc.edu.

M. Di Ventra is with the Department of Physics, University of California, San Diego, La Jolla, California 92093-0319
e-mail: diventra@physics.ucsd.edu.

(which is the time integral of the voltage) are not considered as a separate group since such devices can be redefined in the current-voltage basis [1]. Moreover, we note that memristors, memcapacitors and meminductors are ideal (and rare) instances of memristive, memcapacitive and meminductive systems, respectively (see Refs. [1], [3], [7]). In this work, the terms memristors, memcapacitors and meminductors are reserved only for such ideal cases.

These memory systems turn out to be of very general interest in science and engineering and are potentially useful not just in information storage but also in apparently different areas of research [8], [9], [10], [11], [12], [13], [14], [15], [16], [17], [18], [19], [20], [7]. Of equal importance and arguably the less studied of all these applications so far, memory elements may be of use in the three different paradigms of computation: analog, digital, and quantum. This is the subject of this paper.

In the case of analog computation, it was recently shown that electronic circuits with memory circuit elements [3] can simulate processes typical of biological systems such as the adaptive behavior of unicellular organisms [10], learning and associative memory [16]. The concept of "learning circuits" has also been implemented recently using VO_2 as memory element [20]. Here, we first briefly discuss existing memristive models of neural computing as well as realization of spike-timing-dependent plasticity (STDP) with first-order memristive systems. Then, we formulate a model of a second-order memristive synapse which resembles closer the operation of its biological counterpart.

The implementation of classical logic operations with memristive systems was discussed theoretically in the past (see e.g. Refs. [21], [22], [11]) and demonstrated experimentally [18]. In this paper, we suggest a different scheme for classical logic operations utilizing a combination of memcapacitive and memristive systems. Our scheme realizes all basic logic operations (NOT, OR, AND) as well as many other operations (XOR, multi-input OR, AND, etc.) in a much simpler way as compared to the alternative approaches [11], [18]. In addition, it provides a significant speed-up of operations. In this paper, we demonstrate experimentally for the first time addition of two one-bit numbers using memory circuit elements. Our scheme requires only 16 steps compared to 87 steps as suggested in a previous approach [11]. Also, it is worth stressing that in these cases computing *and* memory are integrated in the *same* platform, which is a major conceptual departure from present-day computing technology where memory and computing are physically disjoint.

Finally, in the case of quantum computation we discuss

Fig. 1. (Color online) (a) A simple neural network containing three electronic neurons (N$_1$, N$_2$ and N$_3$) connected by two memristive synapses (S$_1$ and S$_2$). Reprinted from Ref. [16], copyright (2010), with permission from Elsevier. (b) Change in memristance ΔR induced by a pair of square pulses of opposite polarity applied to terminals of a first-order memristive system described by Eqs. (3, 4) plotted as a function of a time interval between the forward (pre-synaptic) and backward (post-synaptic) pulses $\delta t = t_{post} - t_{pre}$. The pulses' form is shown schematically in the inset (not to scale). The grey rectangle designates the time window in which the memristance change occurs. The maximum pulse overlap is at $\delta t = 0$ and corresponds to the maximum of ΔR. This plot was obtained as a numerical solution of Eqs. (3, 4) with $\alpha = 0$, $\beta = -25$kOhms/(V·s), $V_t = 1.5$V, $R(t = 0) = 2$kOhms, $R_1 = 1$kOhms and $R_2 = 10$kOhms. Pre-synaptic and post-synaptic pulses were selected of ± 1V amplitude and 10ms width.

specific quantum computing schemes where meminductive and memcapacitive systems could be used to generate an essentially infinite number of programmable interaction Hamiltonians between two or more qubits inductively or capacitively coupled, in a manner we could term *field-programmable quantum computation*, the quantum analog of the well-established classical field-programmable gate array. This opens up the possibility of expanding both our fundamental understanding of circuit quantum electrodynamics [23], [24] as well as the optimization of quantum computing algorithms.

II. NEURAL COMPUTATION WITH MEMRISTIVE SYSTEMS

Neuromorphic computing circuits are designed by borrowing principles of operation typical of the human (or animal) brain and, therefore, due to their intrinsic analog capabilities they can potentially solve problems that are cumbersome (or outright intractable) by digital computation. Examples of such problems include - but are not limited to - adaptive behavior, learning by association, pattern recognition, fuzzy logic, etc. Certain realizations of memristive systems can be very useful in such circuits because of their intrinsic properties which mimic to some extent the behavior of biological synapses. In addition, the most recent experimental realizations of memory elements pertain to systems of dimensions in the nanometer regime [25], [26], thus allowing a possible scale-up of such elements in a chip to the number density of a typical human brain (consisting of about 10^{11} synapses/cm^3). In the following we first briefly review our work on *memristive neural networks* (MNNs) showing a practical realization of the Hebbian learning, which states, in a very simplified form, that "neurons that fire together, wire together".

We then discuss one of the most important functions of synapses namely their spike-timing-dependent plasticity [27], [28], [29], [30]. The existing experimental approaches to STDP are based on relatively large-size VLSI circuits [31], [32], [33], [34], three terminal transistor-like structures based on ionic conduction [15] or combination of memristive systems with CMOS elements [19]. Below, we discuss two different memristive system-based schemes in which STDP can be realized. In the first, we may call "bipolar", first-order memristive systems probed by two composite pulses overlapping in time develop STDP. This is similar to what has been studied in [35], [36], [37], [38]. In the second realization, we could call "intrinsic", we provide a model of a memristive system which at the prize of increasing the number of state variables to two, does show STDP even if the excitation pulses do not overlap temporally. This situation is closer to the actual operation of a biological synapse in which each synaptic event triggers a cascade of internal decaying processes/reactions.

A. Memristive neural networks and Hebbian learning

In Fig. 1(a) we show a simple MNN consisting of two memristive systems mimicking the behavior of synapses and three electronic neurons (two input and one output) whose role is to monitor their inputs and send (in both forward and backward directions) signals of a given intensity and shape [16]. This network belongs to a wide class of asynchronous (stochastic)
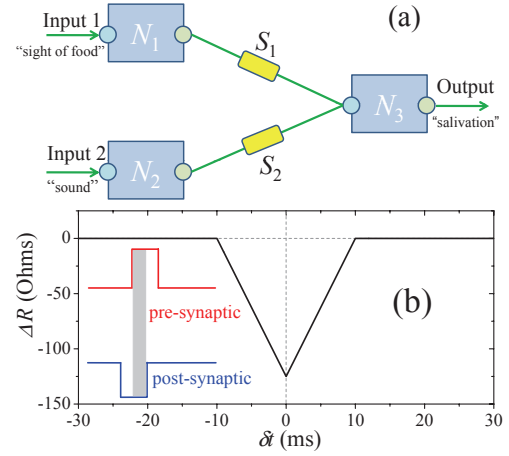
neural networks [39], namely, networks with probabilistic neuron firing. In Ref. [16] we have implemented the behavior of the electronic neurons using an analog-to-digital converter and a microcontroller, so that once the input voltage exceeds a threshold voltage, both forward (of positive polarity) and backward (of negative polarity) pulses are generated whose amplitude is constant, but pulse separation varies according to the amplitude of the input signal. The basic synaptic activity of two electronic synapses (S_1 and S_2 in Fig. 1(a)) has been achieved using memristor emulators [10], [16], [17] pre-programmed with equations of a threshold-type first-order memristive system [10]:

$$I = x^{-1}V_M, \tag{3}$$
$$\dot{x} = (\beta V_M + 0.5(\alpha - \beta)[|V_M + V_t| - |V_M - V_t|]) \\ \times \theta(x/R_1 - 1)\theta(1 - x/R_2), \tag{4}$$

where I and V_M are the current through and the voltage drop on the device, respectively, and x is the internal state variable playing the role of memristance, $R = x$, $\theta(\cdot)$ is the step function, α and β characterize the rate of memristance change at $|V_M| \leq V_t$ and $|V_M| > V_t$, respectively, V_t is a threshold voltage, and R_1 and R_2 are limiting values of the memristance R. In Eq. (4), the θ-functions symbolically show that the memristance can change only between R_1 and R_2. [1]

---

[1]In the actual microcontroller's software implementation, the value of x is monitored at each time step and in the situations when $x < R_1$ or $x > R_2$, it is set equal to R_1 or R_2, respectively. In this way, we avoid situations when x may overshoot the limiting values by some amount and thus not change any longer because of the step function in Eq. (4).
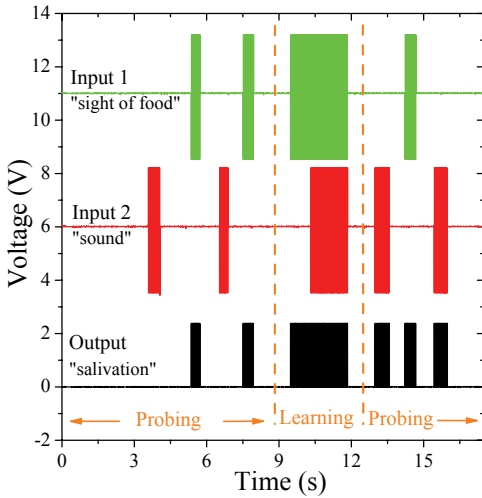
Fig. 2. (Color online) Experimental demonstration of the associative memory with memristive neural networks. In this experiment, a simple neural network shown in Fig. 1(a) was realized. The first "probing" phase demonstrates that, initially, only a signal from N_1 neuron activates the output neuron. The association of the Input 2 signal with the Output develops in the "learning phase" when N_1 and N_2 neurons are simultaneously activated. In this case, a signal at the Input 1 excites the third neuron that sends back-propagating pulses of a negative amplitude. These pulses, when applied simultaneously with forward propagating pulses from the Input 2 to the second memristive synapse S_2 cause it to learn. The final "probing" phase demonstrates that signals from both N_1 and N_2 activate the output neuron. A detailed description of the experiment is given in Ref. [16]. Reprinted from Ref. [16] with modifications, copyright (2010), with permission from Elsevier.

When $\alpha = 0$ and V_t is above the amplitude of the forward (pre-synaptic) pulse but does not exceed its doubled amplitude, the change in memristance (ΔR) is possible only when forward (from N_1 or N_2) and backward (from N_3) pulses overlap. This can be clearly seen if we rewrite Eq. (4) at $\alpha = 0$ (omitting θ-functions) as

$$\dot{x} = \begin{cases} 0 & \text{if } |V_M| \leq V_t, \\ \text{sgn}(V_M)\beta(|V_M| - V_t) & \text{otherwise.} \end{cases} \quad (5)$$

Fig. 1(b) shows the dependence of ΔR on the relative pulse timing. The maximum change of memristance occurs when the pulse overlap is perfect ($\delta t = 0$).

This memristive synapse allows the implementation of the simplest learning rule: Hebbian learning. In fact, if we allow both input electronic neurons to fire at random times, potentiation of the conditioned memristive system S_2 would occur only when the signal of the output neuron N_3 overlaps in time with the signal coming from neuron N_2. In this case, the second synaptic connection S_2 is driven from a high-resistance to a low-resistance state since the voltage drop across S_2 exceeds the threshold value due to the simultaneous excitation of both input neurons (the first one exciting in turn the output neuron). This is shown in Fig. 2 where a detail of this process is described.

B. Spike-timing-dependent plasticity

However, biological synapses show a much more complicated plasticity (with time-resolved properties) [27], [28], [29], [30] than the above simple Hebbian rule seems to
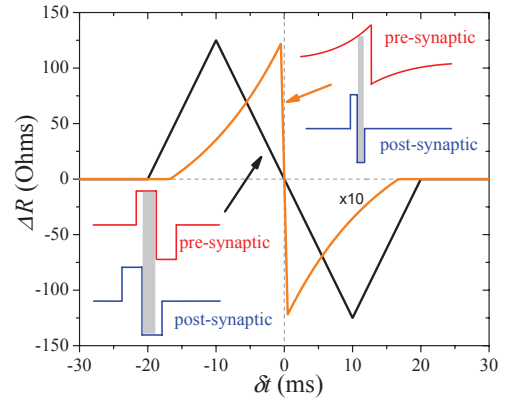

Fig. 3. (Color online) Change in memristance ΔR of a first-order memristive system induced by pair of double pulses (black line) and combination of a non-linear pulse with a double pulse (orange line). The pulse form is shown schematically in the insets (not to scale). The grey rectangles designates the time window in which the memristance change occurs. These curves were obtained as a numerical solution of Eqs. (3, 4) at $\alpha = 0$, $\beta = 25\text{kOhms/(V·s)}$, $V_t = 1.5\text{V}$, $R(t = 0) = 2\text{kOhms}$, $R_1 = 1\text{kOhms}$ and $R_2 = 10\text{kOhms}$. For black curve, each double pulse is composed by a 10ms-wide 1V amplitude pulse immediately followed by 10ms-wide -1V amplitude pulse. For orange curve, the rectangular double pulse is composed by a 0.5ms-wide 1V amplitude pulse immediately followed by 0.5ms-wide -1V amplitude pulse. The non-linear pulse is described by $V_p = V_0 \exp(t/t_0)\theta(-t) - V_0 \exp(-t/t_0)\theta(t)$ with $V_0 = 1.5\text{V}$ and $t_0 = 15\text{ms}$.

suggest. In fact, when a post-synaptic signal reaches the synapse *before* the action potential of the pre-synaptic neuron, the synapse shows long-term depression (LTD), namely its strength decreases (smaller connection between the neurons) depending on the time difference between the post-synaptic and the pre-synaptic signals. Conversely, when the post-synaptic action potential reaches the synapse *after* the pre-synaptic action potential, the synapse undergoes a long-time potentiation (LTP), namely the signal transmission between the two neurons increases in proportion to the time difference between the pre-synaptic and the post-synaptic signals. These general features can be implemented using different types of memristive systems.

1) STDP with first-order memristive systems: The spike-timing-dependent plasticity with first-order memristive systems can be achieved by application of bipolar pulses corresponding to pre-synaptic and post-synaptic action potential pulses. In order to achieve STDP on time scales similar to those encountered in biological synapses, the pulse width should be of the order of 20ms since the memristance modification with this type of memristive systems is possible only during pulses overlap. Fig. 3 demonstrates modification of memristance induced by a pair of rectangular double pulses and also shows the effect of a non-linear and rectangular double pulse on the memristance R. In both cases we observe memristance changes only in a finite time window. Although rectangular double pulses are easier to generate, the use of a non-linear pulse demonstrates a closer similarity of memristance change to the variation of synaptic strength in biological systems.

We also note that the approach to synaptic plasticity using

wide pulses may require reconsideration of rules governing the neural network operation. For example, it is not quite clear how to model multiple pre-synaptic pulses that are fired with a time interval shorter than their pulse length. In this publication, we are not going to focus on such issues and discuss only possible realizations of STDP with memristive synapses.

2) STDP with second-order memristive systems: Having discussed spike-timing-dependent plasticity with first-order memristive systems, let us consider STDP with higher-order memristive systems. The advantage of using higher-order memristive systems is related to their multiple state variables that can make the operation of an artificial synapse closer to the operation of its biological counterpart. In particular, we will focus on second-order memristive systems whose internal state, by definition [2], [3], is described by two state variables. In our model given below, the second state variable y is used to track the time separation between pre-synaptic and post-synaptic action potential pulses.

We consider a second-order memristive system described by the following equations

$$I = x^{-1} V_M, \tag{6}$$

$$\dot{x} = \gamma \Big[\theta(\tilde{V}_M - 1)\theta(\tilde{y} - 1) + \\ \theta(-\tilde{V}_M - 1)\theta(-\tilde{y} - 1) \Big] y, \tag{7}$$

$$\dot{y} = \frac{1}{\tau} \Big[-V_M \theta(\tilde{V}_M - 1)\theta(1 - \tilde{y}) - \\ V_M \theta(-\tilde{V}_M - 1)\theta(\tilde{y} + 1) - y \Big], \tag{8}$$

where x and y are internal state variables, γ is a constant, $\tilde{V}_M = V_M/V_t$, $\tilde{y} = y/y_t$ V_t is a threshold voltage, y_t is a threshold value of y, τ is a constant defining the time window of STDP. It is assumed that short (e.g., $\sim$ 1ms width) pre-synaptic and post-synaptic square pulses of the same polarity are applied to the second-order memristive system. According to Eq. (7), the memristance can change when $|y| \geq y_t$. The change of y is described by Eq. (8) whose right-hand side contains excitation terms involving θ-functions and a relaxation term $-y/\tau$. Therefore, after being excited, the decay of the variable y occurs with a decay constant τ. The particular combination of θ-functions in this equation defines the excitation rules: i) the excitation is possible only when $|V_M| > V_t$ and ii) the variable y excited by a certain polarity of the voltage applied to the memristive system (V_M is given by a difference of pre-synaptic and post-synaptic potentials) can not be re-excited by a pulse of opposite polarity if $|y| > y_t$. We also note that the change in memristance described by Eqs. (6-8) is unconstrained as we are interested only in small changes in R. The constraints on the minimal and maximum values of R can be introduced as it is done in Eqs. (3-4).

A numerically calculated change in memristance as a function of the time interval between the pulses is shown in Fig. 4. This plot is very similar to synaptic weight changes observed in experiments with biological synapses [27], [28], [29], [30] thus lending support to this type of model.

The use of second-order memristive systems in memristive neural networks is very promising since neuron's firing can be implemented simply by short single rectangular pulses with
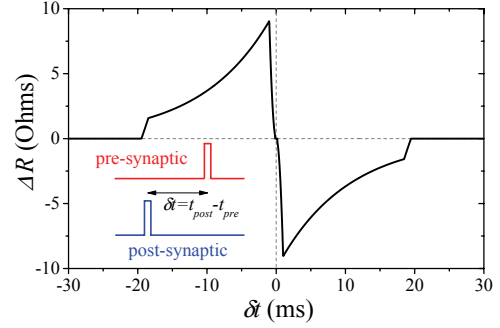

Fig. 4. (Color online) Change in memristance ΔR of the second-order memristie system described by Eqs. (6-8) induced by a pair of rectangular pulses separated by a time interval δt. The pulse form is schematically shown in the inset. This plot was obtained as a numerical solution of Eqs. (6-8) with the following set of parameters: $\gamma = 10^5 \mathrm{C}^{-1}$, $\tau = 1$ms, V_t=0.9V, $y_t = 15$mV, $y(t = 0) = 0$, $x(t = 0) = 2$kOhms. The applied square pulses were of 1V amplitude and 1ms width.

no additional hardware, which is instead needed, for example, to obtain this type of functionality with only first-order memristive systems (as in Ref. [19]). However, such solid-state second-order memristive systems need to be developed, even though their implementation in memristor emulators [10], [16], [17] is straightforward. Moreover, we would like to mention that Eqs. (6-8) provide one of the simplest possible models of second-order memristive systems exhibiting STDP. For instance, abrupt θ-functions entering these equations can be replaced by sigmoidal functions thus providing a smoother analytical behavior.

III. LOGIC GATES AND ARITHMETICS WITH MEMORY CIRCUIT ELEMENTS

In this section, we discuss logic and arithmetic operations performed by the circuit shown in Fig. 5 which comprises an array of memristive systems, a memcapacitive system, a load resistor and drivers. In this type of application, each memristive system is used in the "digital" mode of operation, namely only one bit of information is encoded in the memristor's state. We call "1" (ON) the state of lower resistance and "0" (OFF) that of higher resistance. The operation of the circuit sketched in Fig. 5 relies on charging a memcapacitive system through input memristive system and subsequent discharging through the output ones. In this way, the basic logic operations (NOT, OR, AND) as well as many other operations (XOR, multi-input OR, AND, etc.) are realized in a much simpler fashion than in existing approaches based on memristive systems only [11], [18]. More complex operations (e.g., addition) can be performed by sequences of the elementary logic operations mentioned above.

Using four memristor emulators [17], [16], [40], we have built the circuit described in Fig. 5 and used it to demonstrate the full set of basic Boolean logic operations as well as addition of two one-bit numbers. The extension of such a circuit to operations with multi-bit numbers is straightforward and is not reported here. In fact, the addition of two n-bit numbers in this architecture requires $3n + 1$ memristive systems ($2n$ memristive systems are used to store initial values,
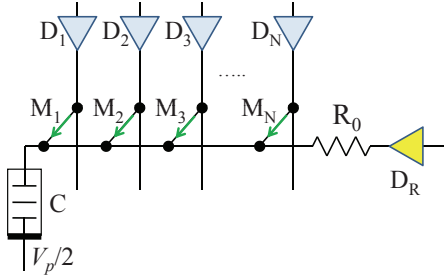
Fig. 5. (Color online) Electronic circuit for Boolean logic and arithmetic operations. In this circuit, an array of N memristive systems M_i, memcapacitive system C and resistor R_0 are connected to a common (horizontal) line. The circuit operation involves charging the memcapacitive system C through input memristive systems and discharging it through the output ones. Because of the circuit symmetry, each memristive system can be used as input or output. From the opposite (top) side, memristive systems are driven by 3-state (0V, V_p, not connected) drivers. The right 4-state (0V, $V_p/2$, V_p, not connected) driver D_R connected through a resistor to the common line is used to initialize memristive systems and memcapacitive system. This scheme employs threshold-type bipolar memristive systems assuming that the application of positive voltage to the top memristor electrode and 0V to the bottom electrode switches memristive system from low resistance state (1 or ON) to the high resistance state (0 or OFF). It is also assumed that the memristor systems' threshold voltage V_t is between $V_p/2$ and V_p.

n memristive systems are reserved for the calculation result and 1 memristive system is used as a carry flag). In the circuit shown in Fig. 5 the initial values are not destroyed and can be reused later. The circuit uses three-state drivers (with voltage states: 0V, V_p, not-connected) connected to memristive systems, and four-state driver (0V, $V_p/2$, V_p, not-connected) connected to the resistor R_0.

Although memcapacitor (as well as meminductor) emulators can also be built using simple electronic schemes [40], [41], their models are not yet well developed. Moreover, the noise reduction is a very important task in experiments with such schemes [40]. Therefore, in our circuit realization we have employed a usual 10μF capacitor in place of the memcapacitive system. We will later discuss the advantages of replacing the regular capacitor with a memcapacitor.

In order to understand the circuit operation, we first note that the circuit employs threshold-type bipolar memristive systems such as the TiO_2 memristive systems recently demonstrated experimentally [4]. To represent this situation we have implemented the equations (3) and (4) in our memristor emulator [10], [16], [17]. In this case, the change of memristance occurs only if the applied voltage exceeds the threshold voltage V_t of the device. In addition, for successful circuit operation, the value of V_t should be selected between $V_p/2$ and V_p. In this case, the charging of C from the completely discharged state will never alter the value of input memristive systems (since during this process voltages applied to input memristive systems do not exceed $V_p/2$).

The circuit operation consists of a sequence of the following elementary operations: 1) capacitor initialization (by application of $V_p/2$ voltage pulse by D_R driver), 2) initialization of memristive systems' states (by application of 0 or V_p voltage pulse by D_R driver simultaneously with V_p or 0 voltage pulse by one of D_1-D_4 drivers), 3) capacitor charging through an
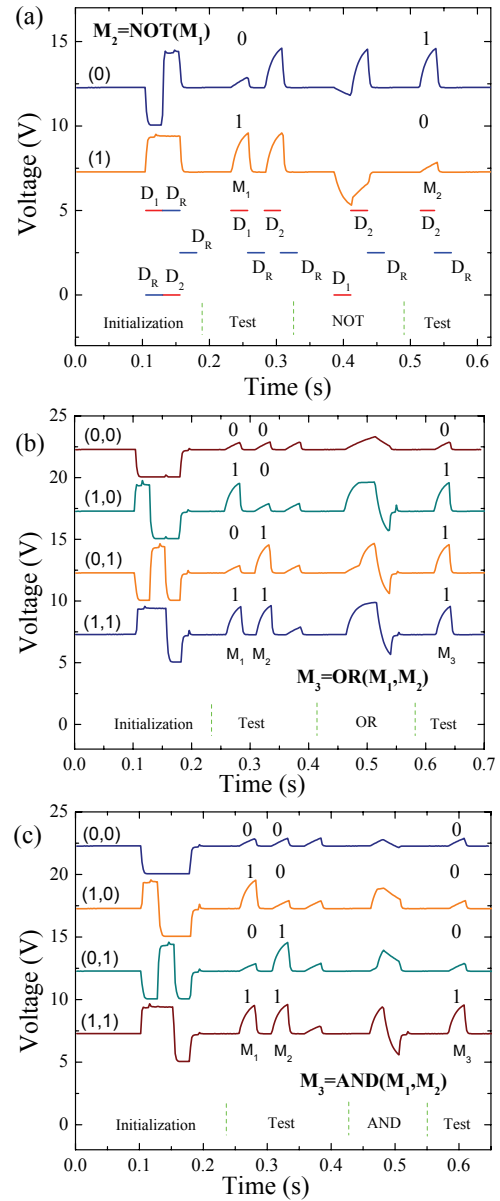

Fig. 6. (Color online) Experimental realization of the basic logic gates with memristive systems based on the circuit shown in Fig. 5 with a capacitor $C = 10\mu$F instead of a memcapacitive system. In our experimental circuit, the role of memristive systems is played by memristor emulators [17], [16], [40] governed by the threshold-type model of Eqs. (3) and (4) with the following set of parameters: $V_t = 4$V, $\alpha = 0$, $\beta = 62$MOhms/(V·s). Each plot shows several measurements of the voltage between the top plate of the capacitor (the common line defined in the caption of Fig. 5) and ground taken for different possible states of input memristive systems. The curves are labeled according to the input values. The detailed information about applied pulse sequences is given in the text. In the bottom of (a) we also show an example of voltages applied to the drivers to generate the top voltage plot (0). Here, we show only voltages applied by drivers, namely, the voltages when a driver is not in "not connected" state. The voltages on the drivers in (a) are in absolute values while the other curves were vertically displaced for clarity.

input memristive system (by application of 0 or V_p voltage pulse by one of the D_1-D_4 drivers), and 4) capacitor discharge through an output memristive system (by application of V_p or 0 voltage pulse by one of D_1-D_4 drivers). Note, that in the operations used by us the current can flow only through one memristive system at any one time. Namely, after the
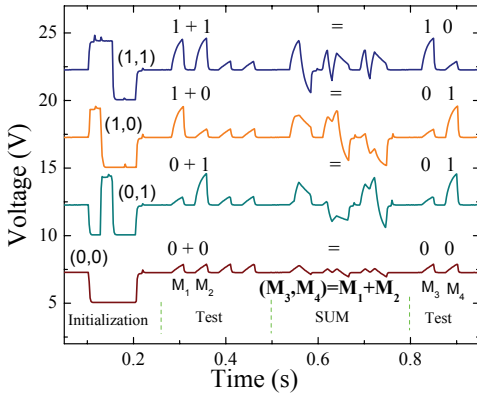
Fig. 7. (Color online) Summation of two one-bit numbers performed as two logic operations: M_3=AND(M_1,M_2) and M_4=XOR(M_1,M_2). The voltage curves corresponding to different values of input numbers have been vertically displaced for clarity.

capacitor has been charged through the input memristive system, the latter is disconnected (its driver is switched into "not connected" state) and the output memristive system is connected to allow capacitance discharge. [2] The parameter values specific to our circuit realization are: $V_p = 5$V, $V_t = 4$V, and 25ms is the width of initialization and reset pulses. An example of sequences of voltage drivers necessary to create the NOT gate is shown in Fig. 6(a). Having discussed elementary circuit operations, let us now turn to implementation of basic Boolean operations.

NOT gate - M_2 = NOT(M_1) - 4 steps - This operation is realized according to the following sequence of operations (see also Fig. 6(a)): set $M_2 = 1$, reset C, charge C through M_1 by 0V pulse of a finite width applied by D_1, discharge C through M_2 by V_p pulse applied to D_2. The main idea is that the capacitor C can only be charged to a sufficiently high voltage to switch M_2 to zero if $M_1 = 1$. Therefore, if $M_1 = 1$ then $M_2 \rightarrow 0$ and if $M_1 = 0$ then $M_2 = 1$. This is the logical NOT operation.

Going into measurement details, in the initialization phase (Fig. 6(a)) we set $M_2 = 1$ and $M_1 = 0$ (top curve (0)) or $M_1 = 1$ (curve (1)) by application of 25ms pulses by D_1, D_2 and D_R drivers as described above. In the first testing phase, we monitor the memristance of M_1 and M_2 by consecutive application of positive 25ms pulses by D_1 and D_2 drivers to corresponding memristive systems as well as capacitor reset pulses. In this way, C is charged through the memristive systems and the charging rate provides information about memristive systems' states. Then, we reset C, charge C through M_1 by 25ms 0V pulse, discharge C through M_2 by 25ms V_p pulse. In the final testing phase, the value of M_2 is monitored via the rate of the capacitor charging, again via application of a 25ms V_p pulse to M_2. If the voltage across the capacitor does not change much then the state of M_2 is 0: high-resistance state and thus low current flows to the capacitor plates. Conversely, if the voltage across the capacitor does change faster to V_p then the state of M_2 is 1: low-resistance state and thus more charges accumulate on the capacitor plates.

[2] Note that the switching of driver states can be done very fast.

For the purpose of clarity, the sequence of applied pulses is shown in the bottom of Fig. 6(a) in absolute scale for the realization of the top sequence of Fig. 6(a). All other curves are shifted for clarity.

OR gate - M_3 = OR(M_1,M_2) - 5 steps - This is implemented by the following sequence: $M_3 = 0$, reset C, charge C through M_1 by V_p pulse, charge C through M_2 by V_p pulse, discharge C through M_3 by 0V pulse. The width of all pulses in this sequence is 25ms. Figure 6(b) shows four voltage lines corresponding to different initial states of M_1 and M_2 memristive systems. The correct truth table of the OR gate is clearly identified during the second testing phase in Fig. 6(b).

AND gate - M_3 = AND(M_1,M_2) - 5 steps - The sequence for this logic gate is as follows: $M_3 = 0$, reset C, charge C through M_1 by a short V_p pulse, charge C through M_2 by a short V_p pulse, discharge C through M_3 by 0V pulse. In the AND operation, the width of short pulses is equal to 10ms and the width of all other pulses is 25ms. The width of short charging pulses is selected in such a way that both M_1 and M_2 memristive systems should be in the ON state in order to charge C to such a voltage so that during the next step, namely during the capacitor discharge through M_3, the latter is switched into the ON state. Fig. 6(c) shows results demonstrating correct implementation of the AND gate.

XOR gate - M_3 = XOR(M_1,M_2) - 11 steps - This is realized by the following sequence: $M_3 = 0$, reset C, charge C through M_1 by a short V_p pulse, discharge C through M_2 by a short 0V pulse, charge C through M_1 by a short V_p pulse, discharge C through M_3 by 0-V pulse, reset C, charge C through M_2 by a short V_p pulse, discharge C through M_1 by a short 0V pulse, charge C through M_2 by a short V_p pulse, discharge C through M_3 by 0-V pulse. Similarly to the AND gate, the duration of short pulses is 10 ms and that of all other pulses is 25 ms.

Addition of two 1-bit numbers - 16 steps - Next, we consider the addition of two one-bit numbers that we encode in M_1 and M_2 memristive systems. The result of addition is saved in M_3 and M_4 memristive systems. It is easy to check that the addition can be performed with the sequence M_3=AND(M_1,M_2) and M_4=XOR(M_1,M_2). In Fig. 7 we show experimentally measured signal patterns that prove the above operation. We emphasize that an approach suggested previously [11] would require 87 steps to perform the same operation.

At this point, we would like to re-emphasize that the extension of our scheme to the addition of n-bit numbers is straightforward. In particular, the i-th bit of the result will be given by a sum of the two i-th bits of the input numbers and the carry flag, from the summation of the i-1 bits. In the case of the one-bit addition considered in the present work, the carry flag is encoded in the M_4 memristive system. Moreover, we want to stress that the circuit operation can be further optimized if we use a memcapacitive system as shown in Fig. 5 (instead of the usual capacitor implemented here). In this case, the state of the memcapacitive system can evolve when pulses are applied to those memristive systems that store the initial values. Therefore, some computation results can be temporarily stored in the memcapacitive system state thus decreasing the number of computation steps required.
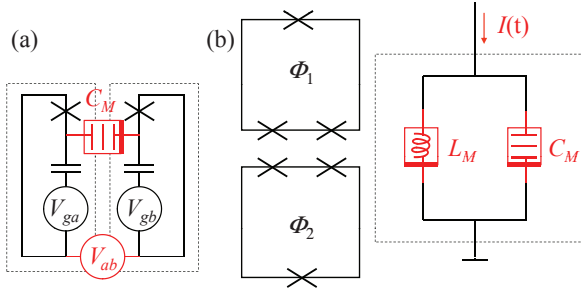
Fig. 8. (Color online) (a) Suggested coupling of charge qubits using a memcapacitive system C_M. Here, V_{ab} is a controllable voltage source used to set the state of the memcapacitive system, while V_{ga} and V_{gb} are voltage sources needed to control the number of electrons across the Josephson junction represented by the cross sign. (b) Suggested coupling of flux qubits using a tank circuit with a meminductive system, L_M and a memcapacitive system, C_M. Here, Φ_1 and Φ_2 are the fluxes that are controlled by the current flowing in the tank circuit and possibly by other controlling coils.

Finally, we would like to mention that the crossbar architectures - formed by "vertical" and "horizontal" sets of wires - typically used to fabricate nanoscale memristive systems [25], [26], [13] may allow an effective parallelization of the arithmetic and logic operations we have described here. For instance, the application of pulses to "vertical" wires would cause a computation within each horizontal line in parallel. Moreover, switching the role of horizontal and vertical wires would cause a switch of computation direction. In this way, interesting and more complex computational schemes can be practically realized. However, a practical realization of such a scheme may require use of highly nonlinear memristive systems or additional switches/individual access devices in order to avoid unwanted currents that naturally appear in a resistive network. In addition, if unwanted currents can be eliminated or reduced, this massive parallelization may offset intrinsically slower switching times of memristive systems ($\gtrsim$ 10ns) in comparison with typically shorter switching times of, e.g., CMOS-based elements performing arithmetic operations.

IV. QUANTUM COMPUTATION WITH MEMORY ELEMENTS

It seems timely to consider the potentialities of memory elements - in particular low-dissipative meminductive and memcapacitive systems - in quantum computation, which is based on the unitary evolution of a quantum system. Although many experimental systems have been suggested as quantum bits (qubits) [42], [43], [44], [45], [46], here we will focus on superconducting (SC) qubits [46], [47] that currently are considered among the most promising ones. Since typical SC qubit circuits involve capacitors and inductors, memcapacitive and meminductive systems fit naturally in this application.

Field-programmable quantum computation - In SC quantum computation schemes, phase and charge qubits are coupled capacitively while flux qubits are coupled inductively [47]. Memcapacitive and meminductive systems can be used in such schemes to provide a controllable interaction between

SC qubits [3]. For example, let us consider two charge qubits [50], [51] interacting via a usual capacitive coupling. The corresponding coupling term has the form [47]

$$H_{int} = \frac{e^2}{2C_x}\sigma_a^x\sigma_b^x, \qquad (9)$$

where e is the elementary charge and $\sigma_{a(b)}^x$ are the x-component Pauli matrices acting on the wave function of the corresponding qubit in the reduced Hilbert subspace. We can now replace the capacitor C_x by a memcapacitive system C_M and insert a controllable voltage source V_{ab} between the qubits (see Fig. 8(a)). Alternatively, V_{ab} can be directly connected in parallel with the memcapacitive system. This last scheme, however, may induce large currents in the two qubits if the qubits circuits are grounded thus perturbing them incoherently. Either way, the value of the memcapacitance - that replaces C_x in Eq. (9) - can be *pre-set* and the interaction Hamiltonian will depend on this pre-set value of capacitance. For two interacting qubits the magnitude of the interaction strength is not very important as it can be compensated by the interaction time. However, if we consider N simultaneously interacting qubits then a variation of coupling between two of them will result in absolutely different interaction Hamiltonians thus leading to a different system evolution. Quantum computation algorithms will thus benefit from such novel quantum hardware functionality because of the many (practically infinite) interaction schemes that can be implemented within a single device architecture.

In the case of flux qubits the latter can be controlled, via mutual inductance, by a tank circuit consisting of a meminductive system with a regular capacitor or possibly a memcapacitive system as shown in Fig. 8 (b). The tank circuit may be current- or voltage-controlled and by setting the different values of meminductance, L_M and memcapacitance, C_M, its frequency $\omega = 1/\sqrt{L_M C_M}$ changes thus leading to a different interaction Hamiltonian between the two qubits. Again, in the case of N interacting qubits this leads to a large number of time evolutions and thus different computation schemes. Because of the similarity to classical field-programmable gate arrays, we could term the above two computation architectures as "field-programmable quantum computation". Some work is however needed to realize such an architecture practically, in particular, to avoid additional decoherence effects that can be introduced by real memcapacitive/meminductive elements [52], [53], [12], [54], [55], [56].

V. CONCLUSIONS

In conclusion, we have addressed all three different paradigms of computation - neuromorphic (analog), digital and quantum - and shown the potential the three classes of memory elements, namely memristive, memcapacitive and meminductive systems offer in all three cases. In particular,

[3]The range of possible applications of memory elements in quantum computing is not limited to this situation, and we indeed anticipate many other different opportunities. For instance, a micromechanical resonator embedded into a DC SQUID [48] results in an effective meminductive system. In addition, a lagging of SC qubits due to memory effects in inductance was recently discussed [49].

we have discussed memristive neural networks, classical logic and arithmetic operations with memristive and memcapacitive systems, and field-programmable quantum computation with meminductive and memcapacitive systems with both charge and flux qubits. Clearly, much work needs to be done to advance these applications. Important issues include, e.g., realization of high connectivity in neural networks (each neuron in the human brain has $\sim$ 7000 synaptic connections), effective parallelization of logic and arithmetic operations, reduction of qubit decoherence, etc. In spite of these difficulties, with the increasing research into actual materials and devices that behave as memory elements we anticipate many more ideas could be implemented in actual systems and circuits thus offering a wider range of opportunities even in hybrid computational schemes involving any two, or even all three paradigms.

ACKNOWLEDGMENT

REFERENCES

[1] L. O. Chua, "Memristor - the missing circuit element," *IEEE Trans. Circuit Theory*, vol. 18, pp. 507–519, 1971.
[2] L. O. Chua and S. M. Kang, "Memristive devices and systems," *Proc. IEEE*, vol. 64, pp. 209–223, 1976.
[3] M. Di Ventra, Y. V. Pershin, and L. O. Chua, "Circuit elements with memory: Memristors, memcapacitors, and meminductors," *Proc. IEEE*, vol. 97, no. 10, pp. 1717–1724, 2009.
[4] J. J. Yang, M. D. Pickett, X. Li, D. A. A. Ohlberg, D. R. Stewart, and R. S. Williams, "Memristive switching mechanism for metal/oxide/metal nanodevices," *Nat. Nanotechnol.*, vol. 3, pp. 429–433, 2008.
[5] Y. V. Pershin and M. Di Ventra, "Spin memristive systems: Spin memory effects in semiconductor spintronics," *Phys. Rev. B*, vol. 78, p. 113309, 2008.
[6] X. Wang, Y. Chen, H. Xi, H. Li, and D. Dimitrov, "Spintronic memristor through spin-torque-induced magnetization motion," *El. Dev. Lett.*, vol. 30, pp. 294 – 297, 2009.
[7] Y. V. Pershin and M. Di Ventra, "Memory effects in complex materials and nanoscale systems," *Advances in Physics*, vol. 60, pp. 145–227, 2011.
[8] P. Kuekes, D. Stewart, and R. Williams, "The crossbar latch: Logic value storage, restoration, and inversion in crossbar circuits," *J. Appl. Phys.*, vol. 97, p. 034301, 2005.
[9] T. Driscoll, H.-T. Kim, B. G. Chae, M. Di Ventra, and D. N. Basov, "Phase-transition driven memristive system," *Appl. Phys. Lett.*, vol. 95, pp. 043 503–1–043 503–3, 2009.
[10] Y. V. Pershin, S. La Fontaine, and M. Di Ventra, "Memristive model of amoeba learning," *Phys. Rev. E*, vol. 80, pp. 021 926–1–021 926–6, 2009.
[11] E. Lehtonen and M. Laiho, "Stateful implication logic with memristors," in *Proceedings of the 2009 International Symposium on Nanoscale Architectures (NANOARCH'09)*, 2009, pp. 33 – 36.
[12] T. Driscoll, H.-T. Kim, B.-G. Chae, B.-J. Kim, Y.-W. Lee, N. M. Jokerst, S. Palit, D. R. Smith, M. Di Ventra, and D. N. Basov, "Memory metamaterials," *Science*, vol. 325, pp. 1518–1521, 2009.
[13] J. Borghetti, Z. Li, J. Straznicky, X. Li, D. A. A. Ohlberg, W. Wu, D. R. Stewart, and R. S. Williams, "A hybrid nanomemristor/transistor logic circuit capable of self-programming," *Proc. Nat. Ac. Sci.*, vol. 106, pp. 1699–1703, 2009.
[14] N. Gergel-Hackett, B. Hamadani, B. Dunlap, J. Suehle, C. Richter, C. Hacker, and D. Gundlach, "A Flexible Solution-Processed Memristor," *IEEE El. Dev. Lett.*, vol. 30, pp. 706–708, 2009.
[15] Q. Lai, L. Zhang, Z. Li, W. F. Stickle, R. S. Williams, and Y. Chen, "Ionic/electronic hybrid materials integrated in a synaptic transistor with signal processing and learning functions," *Adv. Mat.*, vol. 22, p. 2448, 2010.
[16] Y. V. Pershin and M. Di Ventra, "Experimental demonstration of associative memory with memristive neural networks," *Neural Networks*, vol. 23, p. 881, 2010.
[17] ——, "Practical approach to programmable analog circuits with memristors," *IEEE Trans. Circ. Syst. I*, vol. 57, p. 1857, 2010.
[18] J. Borghetti, G. S. Snider, P. J. Kuekes, J. J. Yang, D. R. Stewart, and R. S. Williams, "'Memristive' switches enable 'stateful' logic operations via material implication," *Nature*, vol. 464, pp. 873–876, 2010.
[19] S. H. Jo, T. Chang, I. Ebong, B. B. Bhadviya, P. Mazumder, and W. Lu, "Nanoscale memristor device as synapse in neuromorphic systems," *Nano Lett.*, vol. 10, pp. 1297–1301, 2010.
[20] T. Driscoll, J. Quinn, S. Klein, H. T. Kim, B. J. Kim, Y. V. Pershin, M. Di Ventra, and D. N. Basov, "Memristive adaptive filters," *Apl. Phys. Lett.*, vol. 97, p. 093502, 2010.
[21] D. Strukov and K. Likharev, "CMOL FPGA: a reconfigurable architecture for hybrid digital circuits with two-terminal nanodevices," *Nanotechn.*, vol. 16, pp. 888–900, 2005.
[22] G. S. Snider and R. S. Williams, "Nano/CMOS architectures using a field-programmable nanowire interconnect," *Nanotechnology*, vol. 18, p. 035204, 2007.
[23] A. Blais, R.-S. Huang, A. Wallraff, S. M. Girvin, and R. J. Schoelkopf, "Cavity quantum electrodynamics for superconducting electrical circuits: An architecture for quantum computation," *Phys. Rev. A*, vol. 69, p. 062320, 2004.
[24] A. Wallraff, D. Schuster, A. Blais, L. Frunzio, R. Huang, J. Majer, S. Kumar, S. Girvin, and R. Schoelkopf, "Strong coupling of a single photon to a superconducting qubit using circuit quantum electrodynamics," *Nature*, vol. 431, pp. 162–167, 2004.
[25] J. J. Yang, J. Borghetti, D. Murphy, D. R. Stewart, and R. S. Williams, "A Family of Electronically Reconfiguiable Nanodevices," *Adv. Mat.*, vol. 21, pp. 3754–3758, 2009.
[26] S. H. Jo, K.-H. Kim, and W. Lu, "High-density crossbar arrays based on a si memristive system," *Nano Lett.*, vol. 9, pp. 870–874, 2009.
[27] W. B. Levy and O. Steward, "Temporal contiguity requirements for long-term associative potentiation depression in the hippocampus," *Neuroscience*, vol. 8, pp. 791–797, 1983.
[28] H. Markram, J. Lubke, M. Frotscher, and B. Sakmann, "Regulation of synaptic efficacy by coincidence of postsynaptic APs and EPSPs," *Science*, vol. 275, pp. 213–215, 1997.
[29] G. Q. Bi and M. M. Poo, "Synaptic modifications in cultured hippocampal neurons: dependence on spike timing, synaptic strength and postsynaptic cell type," *J. Neurosci.*, vol. 18, pp. 10 464–10 472, 1998.
[30] R. C. Froemke and Y. Dan, "Spike-timing-dependent synaptic modification induced by natural spike trains," *Nature*, vol. 416, pp. 433–438, 2002.
[31] A. Bofill, A. F. Murray, and D. P. Thompson, "Circuits for VLSI implementation of temporally asymmetric Hebbian learning," in *Advances in Neural Information Processing Systems*, T. G. Dietterich, S. Becker, and Z. Ghahramani, Eds. MIT Press, 2001, vol. 14, p. 1091.
[32] B. Glackin, T. McGinnity, L. Maguire, Q. Wu, and A. Belatreche, "A novel approach for the implementation of large scale spiking neural networks on FPGA hardware," in *Proc. IWANN 2005 Computational Intellingence and Bioinspired Systems*, Barcelona, Spain, June 2005, pp. 552–563.
[33] J. Arthur and K. Boahen, "Learning in silicon: Timing is everything," in *Advances in Neural Information Processing Systems*, B. Sholkopf and Y. Weiss, Eds. MIT Press, 2006, vol. 18, pp. 75–82.
[34] G. Indiveri, E. Chicca, and R. Douglas, "A VLSI array of low-power spiking neurons and bistable synapses with spike-timing dependent plasticity," *IEEE Transactions on Neural Networks*, vol. 17, pp. 211–221, 2006.
[35] G. S. Snider, "Cortical computing with memristive nanodevices," *SciDAC Review*, vol. 10, pp. 58–65, 2008.
[36] A. Afifi, A. Ayatollahi, and F. Raissi, "Stdp implementation using memristive nanodevice in cmos-nano neuromorphic networks," *IEICE El. Express*, vol. 6, pp. 148–153, 2009.
[37] B. Linares-Barranco and T. Serrano-Gotarredona, "Exploiting memristance in adaptive asynchronous spiking neuromorphic nanotechnology systems," *Proc. IEEE-NANO*, pp. 601–604, Jul 2009.
[38] S. Parkin, "Innately three dimensional spintronic memory and logic devices: Racetrack memory and spin synapses," 2010, talk at 2010 MRS SprinG Meeting.

[39] Y. Kondo and Y. Sawada, "Functional abilities of a stochastic logic neural network," *IEEE Trans. Neural Netw.*, vol. 3, p. 434, 1992.

[40] Y. V. Pershin and M. Di Ventra, "Memristive circuits simulate memcapacitors and meminductors," *Electronics Letters*, vol. 46, pp. 517–518, 2010.

[41] ——, "Emulation of floating memcapacitors and meminductors using current conveyors," *Electronics Letters*, vol. 47, p. 243, 2011.

[42] A. Steane, "The ion trap quantum information processor," *J. Phys. B*, vol. 64, p. 623, 1997.

[43] D. Loss and D. P. DiVincenzo, "Quantum computation with quantum dots," *Phys. Rev. A*, vol. 57, p. 120, 1998.

[44] V. Privman and I. D. Vagner, "Quantum computation in quantum-hall systems," *Phys. Lett. A*, vol. 239, p. 141, 1998.

[45] Y. V. Pershin, I. D. Vagner, and P. Wyder, "Indirect hyperfine interaction between nuclear spin qubits in mesoscopic wires and rings," *J. Phys.-Cond. Matt.*, vol. 15, pp. 997–1006, 2003.

[46] J. Clarke and F. K. Wilhelm, "Superconducting quantum bits," *Nature*, vol. 453, p. 1031, 2008.

[47] A. Zagoskin and A. Blais, "Superconducting qubits," *Physics in Canada*, vol. 63, p. 215, 2007.

[48] M. Poot, S. Etaki, I. Mahboob, K. Onomitsu, H. Yamaguchi, Y. M. Blanter, and H. S. J. van der Zant, "Tunable backaction of a dc squid on an integrated micromechanical resonator," *Phys. Rev. Lett.*, vol. 105, p. 207203, 2010.

[49] S. N. Shevchenko, S. H. W. van der Ploeg, M. Grajcar, E. Il'ichev, A. N. Omelyanchouk, and H.-G. Meyer, "Resonant excitations of single and two-qubit systems coupled to a tank circuit," *Phys. Rev. B*, vol. 78, no. 17, p. 174527, Nov 2008.

[50] V. Bouchiat, D. Vion, P. Joyez, D. Esteve, and M. Devoret, "Quantum coherence with a single cooper pair," *Physica Scripta*, vol. T76, p. 165, 1998.

[51] Y. Nakamura, Y. A. Pashkin, and J. S. Tsai, "Coherent control of macroscopic quantum states in a single-cooper-pair box," *Nature*, vol. 398, p. 786, 1999.

[52] I. Zine-El-Abidine, M. Okoniewski, and J. G. McRory, "A tunable RF MEMS inductor," in *Proceedings of the 2004 International Conference on MEMS, NANO and Smart Systems (ICMENS'04)*, 2004, pp. 636–638.

[53] S. Chang and S. Sivoththaman, "A tunable RF MEMS inductor on silicon incorporating an amorphous silicon bimorph in a low-temperature process," *IEEE El. Dev. Lett.*, vol. 27, no. 11, pp. 905–907, 2006.

[54] Q. Lai, L. Zhang, Z. Li, W. F. Stickle, R. S. Williams, and Y. Chen, "Analog memory capacitor based on field-configurable ion-doped polymers," *Appl. Phys. Lett.*, vol. 95, p. 213503, 2009.

[55] J. Martinez-Rincon, M. Di Ventra, and Y. V. Pershin, "Solid-state memcapacitive system with negative and diverging capacitance," *Phys. Rev. B*, vol. 81, p. 195430, 2010.

[56] J. Martinez-Rincon and Y. V. Pershin, "Bistable nonvolatile elastic-membrane memcapacitor exhibiting a chaotic behavior," *IEEE Trans. El. Dev.*, vol. 58, p. 1809, 2011.